D. E. Welch[1], L. M. Hively[1], R. F. Holdaway[1]

STP 1417: 33rd National Symposium on Fatigue and Fracture Mechanics

---

Reference: Welch, D. E., Hively, L. M., and Holdaway, R. F., "**Nonlinear Crack Growth Monitoring,**" *Fatigue and Fracture Mechanics: 33rd Volume, ASTM STP 1417,* W. G. Reuter and R. S. Piascik, Eds., American Society for Testing and Materials, West Conshohocken, PA, 2002.

Abstract

Oak Ridge National Laboratory has developed a new technique to monitor the growth of cracks in structural members, and to predict when failure due to this damage is imminent. This technique requires the measurement of global loadings and local deflections/strains at critical locations to indicate the increasing growth of hidden cracks with sufficient warning time prior to failure to take preventative action to correct the problem or retire the structure before failure. The techniques, as described in the referenced report [*2*] have been proven on a laboratory scale to successfully detect the onset of failure due to fatigue cracking (including cracking of corroded samples), stress corrosion cracking, and low temperature creep crack growth, with a reasonable degree of warning before failure.

Keywords: Fatigue, Hysteresis Energy, Strain Energy, Predictive Maintenance, Reliability

[1]Staff Member, Staff Member, and Staff Supervisor, respectively, Oak Ridge National Laboratory, Engineering Technology Division, Oak Ridge, TN 37831-8066.

Nomenclature

a =coefficient of second order term in quadratic fit of HSE vs fatigue cycles
b =coefficient of first order term in quadratic fit of HSE vs fatigue cycles
c =constant coefficient in quadratic fit of HSE vs fatigue cycles
G_{ic} =Griffith critical strain energy release rate
HSE =Hysteresis strain energy
LCL =Lower control limit
M =Total number of fatigue cycles within moving window of width 2w
N =the total number of fatigue cycles experienced
n =the central point of the moving window, n = M - w
P =Global applied load
s =estimate of sample standard deviation
UCL =Upper control limit
w =Half width of filtering window
x_i =the number of a particular HSE measurement
$\bar{x}$ =the mean value of all HSE measurements up to the current cycle
y =the quadratic fit representation of the HSE value
z =the value used to obtain a quadratic fit of the HSE vs fatigue cycles data about a central point n
d =the local critical deflection in the region of a defect
? =the curvature of the HSE vs fatigue cycles curve

Introduction

During the 1930s, A. A. Griffith introduced the technique of considering crack growth in solids as a process of energy exchange in which external energy is introduced and stored as internal strain energy. During crack growth, which is an energy consuming process, the internal strain energy and any externally introduced energy from loading is transformed into new crack surface area. When the rate of change of internal strain energy per unit crack extension equals the rate of consumption of surface energy due to additional crack surface creation, a crack will begin to extend. This critical strain energy release rate, called G_{Ic}, then becomes a criterion for the onset of initial crack extension. The subscript, I, indicates Mode I crack growth, although the technique is also valid for the other two modes of crack growth, Modes II (in-plane shear) and Mode III (out-of-plane shear).

Since the 1970s, the brittle fracture and fatigue crack growth rates of materials have been measured as material properties, subject to certain environmental conditions. However, a considerable statistical variation (typically a factor of 10) still occurs in these crack growth rates, and the prediction of crack growth rates in various materials and environments has been

very difficult analytically. Loading amplitude and frequency, gaseous and liquid environment, temperature, loading mode (tension, flexure, or shear), and crack growth mode (Mode I, II, or III) all may vary frequently and independently. This makes structural safety management uncertain, requiring large safety factors leading to underutilization of capacity.

Background

The technique proposed here involves Griffith energy absorption measurements for structures under load and subject to cracking, based on the concept of G_{Ic} as the critical strain energy release rate. The Griffith critical strain energy release rate criterion for structural failure by cracking states that a crack will begin to extend when the strain energy released from the structure by relaxation during crack extension exactly equals the consumption of energy demanded by the formation of new surface area. This criterion has been established to be a material property, and is stated as:

$$G_{IC} = \frac{-dU}{da}. \qquad (1)$$

Where

U = the strain energy within the structure at the point of the beginning of crack extension
a = crack length

Using this technique for fatigue loading, the energy input into the local portion of the structure is measured by integrating the global load and a local deflection over a complete loading cycle. For structures which are loaded in the elastic regime (as most structures are), this energy will consist principally of two components. The first is thermoelastic damping. The second is the incremental consumption of new surface energy by a slowly increasing crack size.

Our experiments have shown that the initial crack growth rate is small compared to the damping energy for new undamaged structures. By plotting the total strain energy (energy consumed per fatigue cycle) vs number of cycles, we see an initial relatively constant level of energy consumption due to damping. However, as the internal crack grows larger, the crack growth rate energy consumption component grows larger compared to the constant damping energy component, so that the curve of total energy consumption begins to change noticeably near the end of life. It is this **change** in strain energy rather than the level of strain energy itself which is the indicator of the approach of fatigue failure. Therefore, it may be applied to any structure at almost any time. We have tested the technique in Mode I and Mode III cracking, and for tensile, compressive, flexural, and torsional loadings.

We have established a reliable statistical indicator, which indicates the point at which the end of structural fatigue life is near. This indicator provides an indication of approaching failure at between 1 and 20 percent of fatigue lifetime before structural failure. In 50–60 experiments with steel, aluminum, and fiberglass materials, no false positive indications (indications without being closely followed by structural failure) or false negatives (failure to indicate before fatigue failure) were noted. The technique may be implemented either as a continuous online monitoring system for the structure itself, or as a series of periodic loading tests applied during routine maintenance to measure the response of the structure to standard loadings.

Analytical Methods

The HSE is computed as the loop integral:

$$\mathrm{HSE} = \oint P dd \ . \qquad (2)$$

When measured experimentally, the HSE shows short term variability, or noise, as shown in Fig. 1. The HSE will, in general, depend on load amplitude, material, and other variables. Thus, the value of the HSE alone does not predict failure. Consequently, we use the slope of HSE vs number of cycles and the curvature of HSE vs number of cycles as leading indicators of changes in HSE. We extract smooth trends with a novel, zero-phase, quadratic filter [1–3]. This filter uses a moving window of 2w + 1 points, with the quadratic fit obtained from the trailing 2w points behind the evaluation point. We estimate the trend at the leading evaluation point from a quadratic regression of the trailing 2w + 1 points. We find that a filter window width for adequate smoothing is w = 5% of the total number of loading cycles. The smoothed trend then has the form, $y(z) = az^2 + bz + c$. Here, z = M – n, with M as the successively increasing total number of fatigue cycles to the evaluation point at the end of the moving window, and n as the number of loading cycles associated with the variable trailing point in the filter window. The corresponding value of y(z) at the evaluation point of the window is $y(z = 0) = az^2 + bz + c = c$. The slope at the evaluation point is $y'(z = 0) = 2az + b = b$. The second derivative at the evaluation point of the window is $y''(z = 0) = 2a$. The curvature of the curve $y(z)$ is defined as:

---

[1] L. M. Hively et al., *Nonlinear Analysis of EEG for Epileptic Seizures*, ORNL/TM-12961, Oak Ridge National Laboratory, April 1995.

[2] N. E. Clapp and L. M. Hively, *Method and Apparatus for Extraction of Low-Frequency Artifacts from Brain Waives for Alertness Detection*, U.S. Patent #5,626,145, May 6, 1997.

[3] L. M. Hively et al., *Apparatus and Method for Epileptic Seizure Detection using Nonlinear Techniques*, U.S. Patent #5,743,860, April 28, 1998.

$$k = \frac{y''}{\left[1+(y')^2\right]^{3/2}} \quad . \tag{3}$$

Experimental data shows that considerable low-amplitude variation still exists in the slope and curvature even after this filtering process. Consequently, we distinguish random variations from a systematic trend to detect the onset of failure. We treat the values of slope and curvature as statistical variables, similar to the variables in a process control chart. In the subsequent analysis, $\bar{x}$ denotes the sample mean, which is computed from the beginning of the data to the current cycle:

$$\bar{x} = \frac{\sum_{i=1}^{n} x_i}{n}. \tag{4}$$

The corresponding standard deviation estimate (s) is obtained from

$$s^2 = \frac{\sum_{i=1}^{n} \left(x_i - \bar{x}\right)^2}{N-1}. \tag{5}$$

We define an indication of failure onset as the point when the slope (or curvature) rises above the upper control limit (UCL) or falls below the lower control limit (LCL). These values are defined as:

$$\begin{aligned} \mathrm{UCL} &= \bar{x} + 4s \\ \mathrm{LCL} &= \bar{x} - 4s \end{aligned}. \tag{6}$$

The probability of Gaussian random data exceeding one of these limits corresponds to a false positive probability of approximately 1 part in 31,574 measurements (cycles). This value is chosen as the approximate number of fatigue cycles expected before failure to prevent false positives or false negatives.

Experiments

Objective

Our first series of experiments was designed to record tensile load and tensile strain on tension-tension-loaded aluminum coupons which were designed to simulate multiple site damage (MSD) situations by containing a single No. 55 drilled hole (1.32×10^{-3} m , [.052-in].-diam.) hole in the center of the gage section. The HSE was then calculated for each sample during each fatigue cycle. Then, the techniques of Analytical Methods Section 3 were applied to predict the approach of fatigue failure.

Method

The coupon material was an unclad 2024-T3 aluminum alloy sheet, commonly used in aircraft skins. The coupons were nominally 2.286×10^{-3} m (0.090-in.) thick and were machined to an ASTM E466 standard fatigue specimen with a cross-sectional shape of 0.033 m(1.3-in.) long by 0.0127 m(½-in) wide gage section with a 0.0254 m(1-in.) extensometer across the gage section.

Two variables were recorded: tensile load and strain measured by the extensometer. Loading was performed on a servo hydraulic test machine of 44,480 Nt (10,000) lb capacity and at room temperature. The fatigue loading frequency was 10 Hz. Data were recorded by a National Instruments PCI 16XE-50 General Purpose I/O System with 16-bit resolution. The data recording frequency was 2000/channel/s, producing ~200 measurements of each variable over each fatigue cycle. Load cell voltage variations were of the order of 0.1% (10 mV) of full scale (10 V), or 44.48 Nt (10 lb). Measurement resolution was ~68,950 Pa (1 lb in load, or ~10 psi) in stress measurement, and 5 με in strain measurement.

Test Results

An initial tensile stress vs strain curve for a 2024-T3 aluminum coupon was recorded as shown in Fig. 1. Fig. 2 illustrates the hysteresis strain energy effect, wherein a hysteresis loop occurs during each fatigue cycle, the area of which represents the energy stored in the coupon.

The remaining specimens were numbered TM2-MSD-1 through TM2-MSD-8. These specimens were fatigue tested in tension-tension at R = 0.1, and at the peak nominal stresses shown in (Table 1).

Data Analysis

Typical graphs of the HSE, slope, and curvature for these aluminum samples are shown in (Figs. 3-5).

A specimen was also tested at a number of fatigue stress ranges, and the resulting HSE was measured. The dependence of the plateau HSE value on fatigue stress range was plotted on a log-log plot, and is shown in (Fig. 4). The slope of this line, which is approximately 2, is consistent with the assumption that the initial value being measured is material damping.

Conclusions

These results suggest that, under laboratory conditions, monitoring of the local hysteresis strain energy input into a structure in the vicinity of a local defect by monitoring the loop integral of a quantity proportional to a global loading and a quantity proportional to a local critical deflection can provide a significant forewarning of the approach of tensile fatigue failure. This method has also been demonstrated to operate similarly for structural steel and random chopped mat fiberglass, in other loading modes and crack growth modes, as well as in the presence of simulated corroded conditions, where analytical treatments of crack conditions are very difficult [1].

References

[*1*] Welch, D. E., Hively, L. M., and Ruggles, M. B., *Nonlinear Crack Growth Monitoring*, ORNL-TM-1999/117, Oak Ridge National Laboratory, Oak Ridge, TN October 1999.

[*2*] Clapp, N. E. and Hively, L. E., May 6, 1997, *Method and Apparatus for Extraction of Low-Frequency Artifacts from Brain Waves for Alertness Detection*, U.S. Patent #5,626,145.

[*3*] Hively, L. E. and Ng, E. G., September 29, 1998, *Integrated Method for Chaotic Time Series Analysis*, U.S. Patent #5,815,413.

[*4*] Hively, L. M., et al., January 12, 1999, *Epileptic Seizure Prediction by Nonlinear Methods*, U.S. Patent #5,857,978.

TABLE 1.--*Fatigue test results.*

	Specimen								
	MSD-1a	**MSD-1b**	**MSD-2**	**MSD-3**	**MSD-4**	**MSD-5**	**MSD-6**	**MSD-7**	**MSD-8**
Nominal peak tensile load, lb	780	2,340	2,000	2,000	2,000	2,000	1,500	1,500	1,500
Nominal peak tensile stress, psi	17,333	52,000	44,444	44,444	44,444	44,444	33,333	33,333	33,333
Nominal minimum tensile load, lb	78	234	200	200	200	200	150	150	150
Nominal minimum tensile stress, psi	1,733	5,200	4,444	4,444	4,444	4,444	3,333	3,333	3,333
Cycles to failure	No fail at 10^5	2,550	6,888	5,829	7,923	7,891	27,008	24,180	31,795
Cycles of fatigue life remaining after indication	...	205	649	833	817	1,138	3,307	2,441	3,769
Indication based on slope or curvature	...	Slope	Slope	Slope	Curv.	Curv.	Curv.	Curv.	Curv.
Fatigue life remaining after indication, %	...	8.04	9.42	14.29	10.31	14.42	12.24	10.10	11.85
HSE plateau value	0.07	0.92	0.67	0.62	0.63	0.62	0.31	0.31	0.32

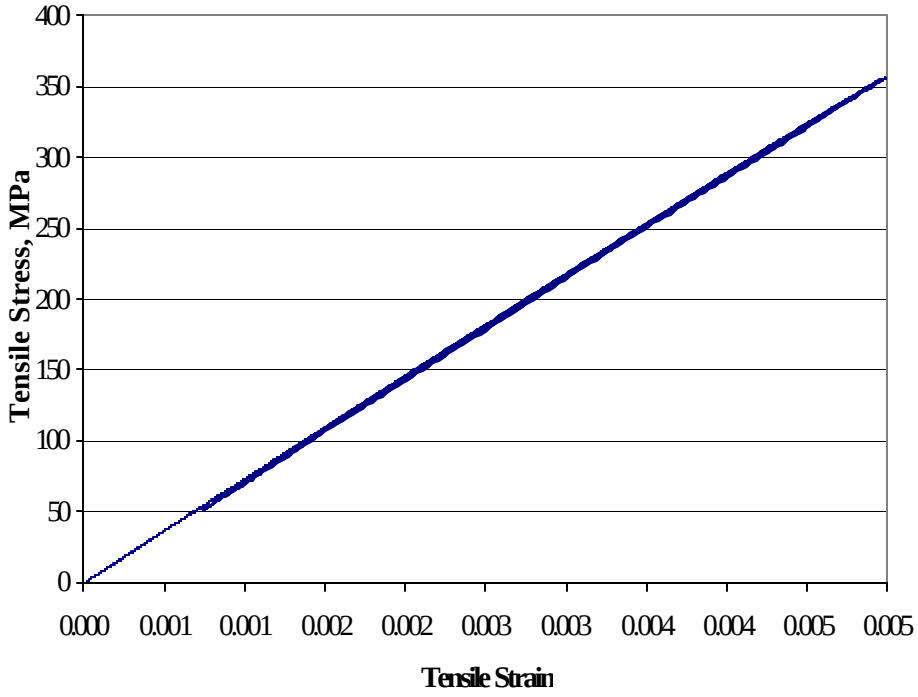

Fig. 1. Initial tensile stress vs strain, unclad 2024-T3 aluminum coupon.

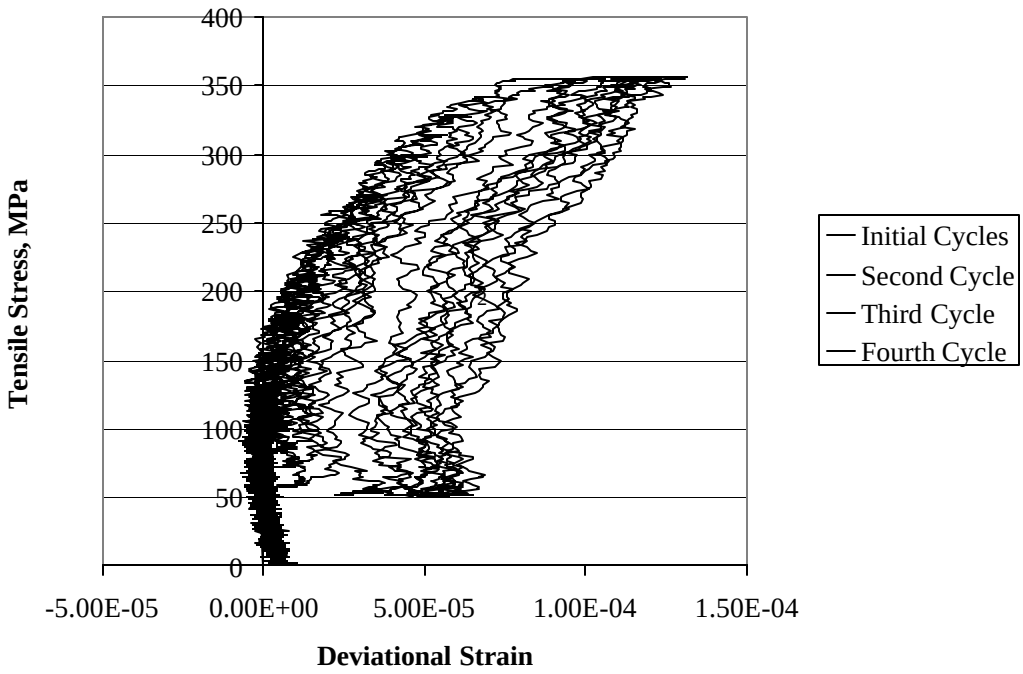

Fig. 2. Tensile stress vs deviational strain, unclad 2024-T3 aluminum coupon.

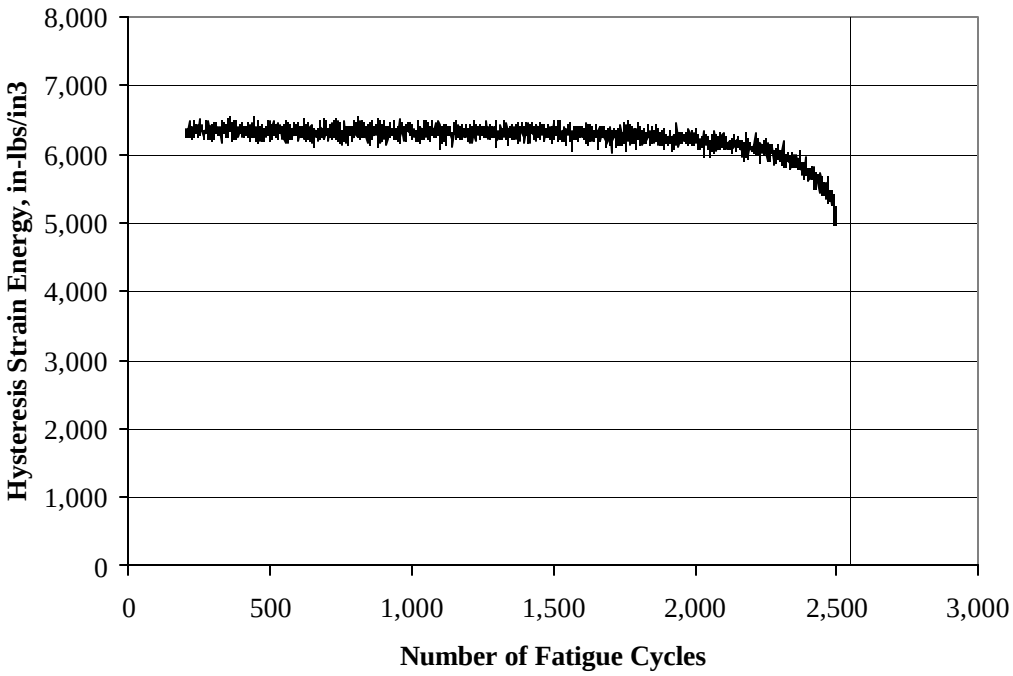

Fig. 3. HSE vs number of fatigue cycles, sample TM2-MSD-1.

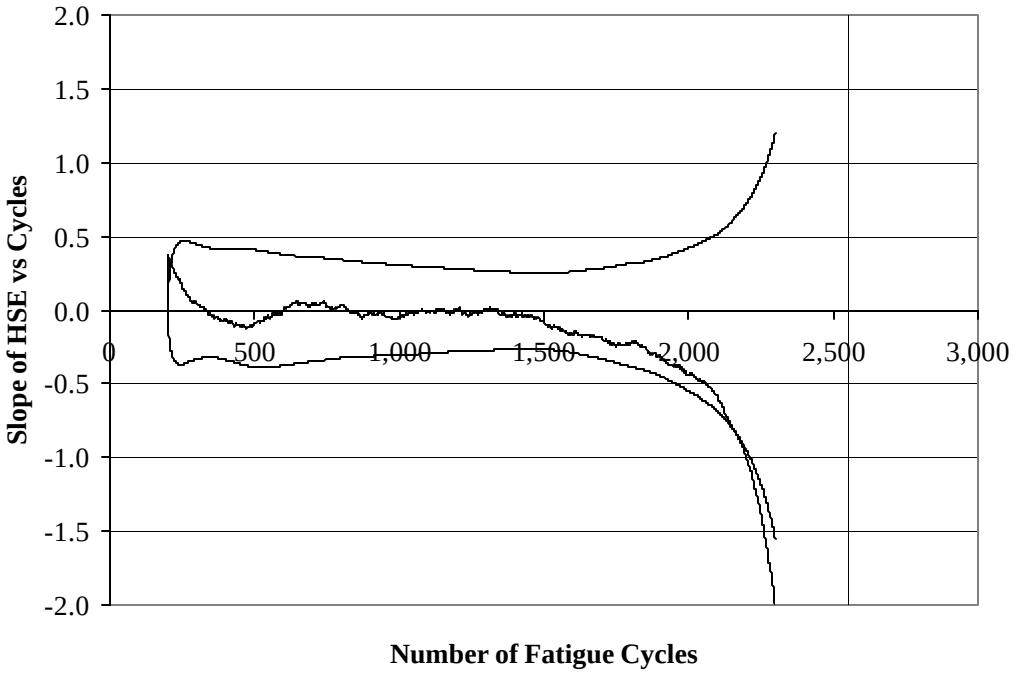

Fig. 4. **Slope of HSE vs number of fatigue cycles, Sample TM2-MSD-1.**

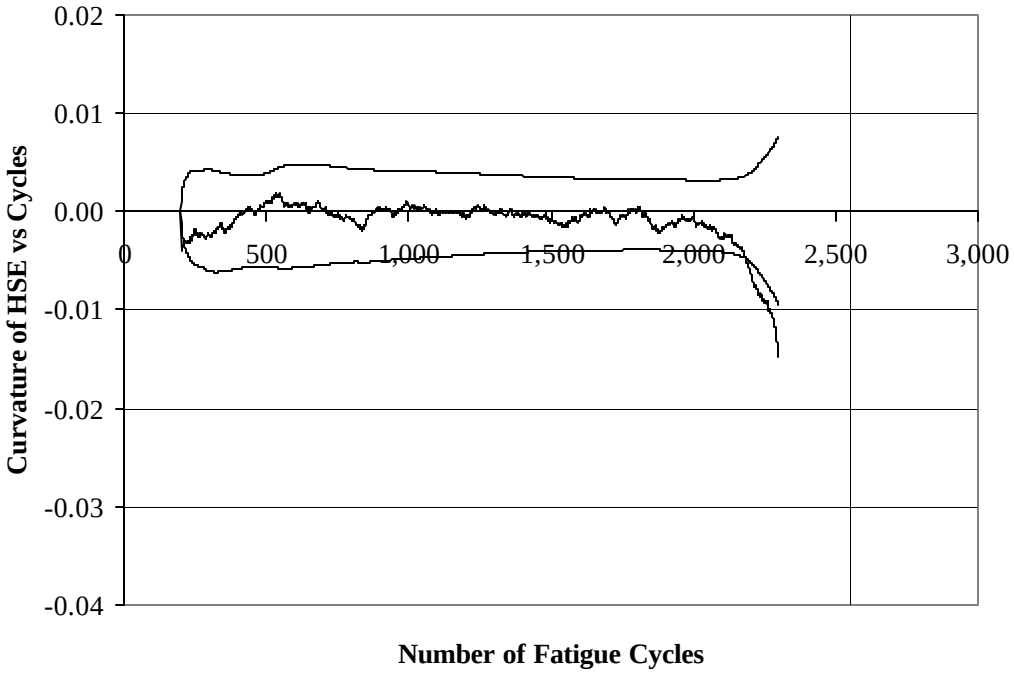

Fig. 5. Curvature of HSE vs number of fatigue cycles, Sample TM2-MSD-1.

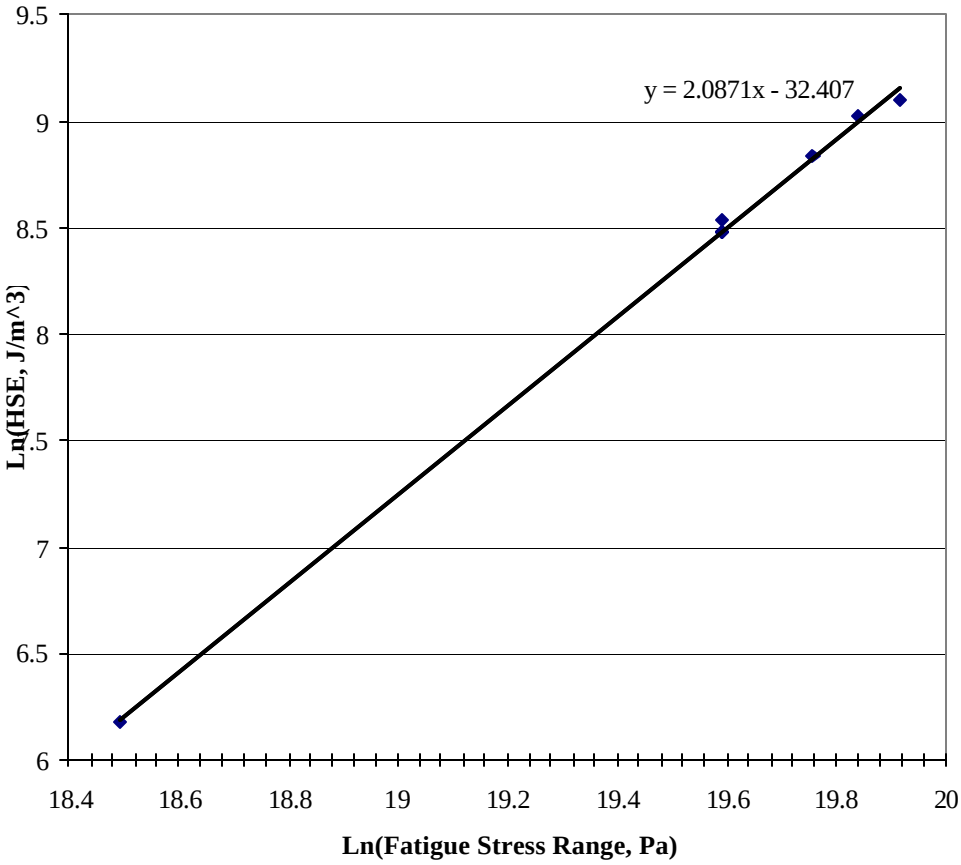

Fig. 6. Log (HSE) vs Log (Fatigue Stress Range), 2024-T3 Aluminum, R=0.1.